

MCNPX MODELING OF HIGH-ENERGY NEUTRON INTERACTIONS IN CsI: CHARGED PARTICLE YIELDS AND PULSE HEIGHT SPECTRA

Thomas D. McLean, Richard H. Olsher and Robert T. Devine

Los Alamos National Laboratory

PO Box 1663, MS J573

Los Alamos, NM, USA

tmclean@lanl.gov, dick@lanl.gov, devine_r@lanl.gov

ABSTRACT

The intrinsic pulse shape discrimination properties of CsI(Tl) form the basis of a portable high-energy neutron (>20MeV) spectrometer currently being developed at LANL. Charged particle spallation products are identified on the basis of pulse shape and sorted into individual pulse height spectra in real time. In order to deconvolute these spectra and reveal the incident neutron spectrum it is vital that the scintillator response functions be well known.

To this end, we have used the high energy physics models (Bertini, ISABEL and CEM2k) embedded in MCNPX to calculate charged particle yields and generate pulse height spectra for incident neutron energies up to 800MeV. We have used the new PHL option for F8 tallies to convert the energy deposited by charged particles into an electron-equivalent light output in order to simulate experimental pulse height spectra.

Recent experimental data obtained at quasi-monoenergetic neutron energies of 33 and 60 MeV at the UCL cyclotron facility has afforded an opportunity to compare theoretical and empirical results. It is shown that at these energies, the CEM2k model gives the best agreement with experimental results with respect to particle yields. However, none of the models are able to adequately describe the pulse height spectra of all the particles of interest.

Key Words: CsI(Tl), MCNPX, Neutron, Spectroscopy

1 INTRODUCTION

There is an on-going program at LANL to develop a portable light weight neutron spectrometer [1] for use in fields above 20MeV such as those found at the LANSCE/WNR (Weapons Nuclear Research) facility. Existing instrumentation such as rem meters are heavy and unable to provide spectroscopic data. In addition, detector response functions with respect to high-energy neutrons are often not well-known leading to large uncertainty in the dose measurement.

The proposed instrument is based on the production and detection of charged particle spallation products in CsI. The well-known pulse shape discrimination properties [2-4] of this scintillator allow real time particle identification, which, in conjunction with the associated pulse height data, yields a 2D map that is neutron energy dependent. Count rate data, combined with crude information from the 2D map, can be used to give a real time conservative indication of neutron dose rates. It is only with recent advances in digital electronics and processor speeds that the proposed instrument has become feasible.

Subsequent off-line unfolding of the pulse shape versus pulse height data can be used to get an accurate representation of the neutron spectrum and hence a better estimate of neutron dose.

However, accurate deconvolution of this data is reliant on a set of response functions that truly describe detector behaviour. This paper describes the calculation of charged particle energy spectra using the high-energy physics models bundled with the MCNPX. These energy spectra have been folded with light curve data to predict pulse height spectra. Experimental pulse height data obtained at the Universite catholique de Louvain (UCL) cyclotron have been compared with these theoretical predictions. MCNPX-predictions of particle yields have also compared with experimental results.

2 FACILITY DESCRIPTION

2.1 Universite Catholique de Louvain

The cyclotron facility at UCL [5] accelerates protons to the requisite energy and directs them to a natural lithium target to generate neutrons via the ${}^7\text{Li}(p,n){}^7\text{Be}$ reaction. Data was recorded at nominal beam energies of 33 and 60 MeV at a distance of 9.6m and an angle of 0 degrees relative to the Li target. Figure 1 shows the quasi-monoenergetic neutron spectra, a characteristic peak centered at the nominal neutron energy and a tail extending to lower energies. These spectra were determined using time-of-flight measurements with a NE213 detector and a ${}^{238}\text{U}$ fission chamber at a reference distance of 11m.

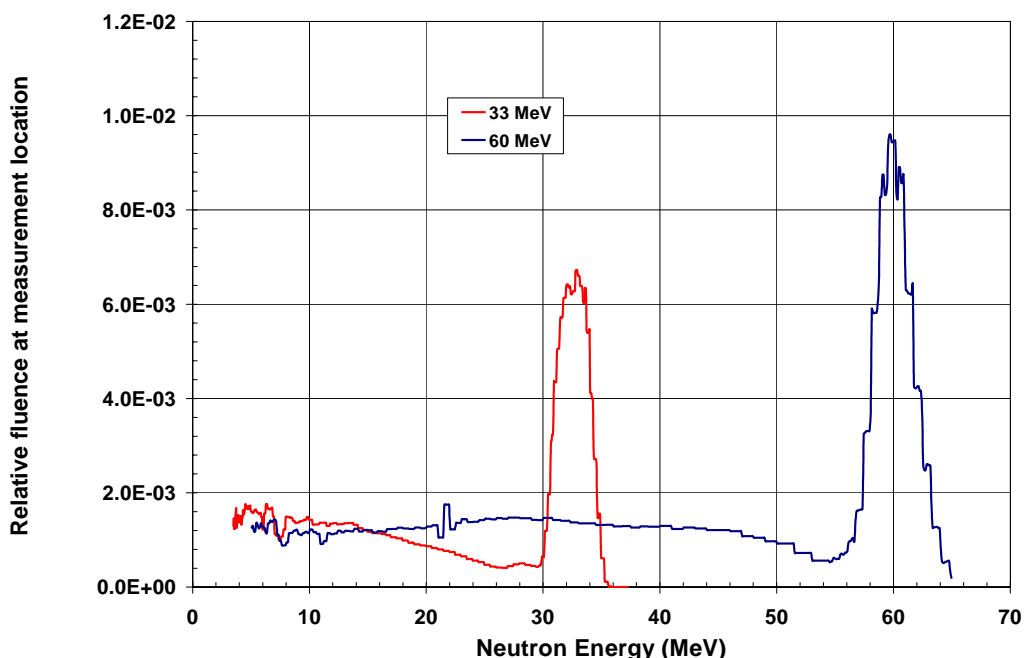


Figure 1. UCL quasi-monoenergetic neutron spectra

Routine beam monitoring during the irradiations was done using a calibrated NE102 plastic scintillator. The uncertainty (1σ) in the total incident fluence was 4% at 33MeV and 5% at 60MeV. Beam currents ranging from 1 to 5 μ A were used.

2.2 LANSCE\WNR

The WNR facility, part of the Los Alamos Neutron Science Center (LANSCE) is used by investigators world wide for basic and applied research. The interaction of 800MeV protons on a tungsten target generates spallation neutrons. The proton beam is typically pulsed at 100Hz with each 625 μ s pulse consisting of a train of micro pulses separated by 1.8 μ s. Typical beam currents average 3.5 μ A.

Beam lines of various lengths radiate from the tungsten target. The beam line used in this study, 4FP15L is offset 15 degrees relative to the target and delivers the hardest available spectrum. To further increase beam hardness, low energy neutrons were preferentially attenuated using a beam in-line filter composed of 4 inches of copper and polyethylene.

The shape of the continuous neutron spectrum was determined using a ^{238}U fission chamber where each fission event was tagged with time-of-flight (TOF) data. Unfolding the TOF spectrum yielded the neutron spectrum shown in Figure 2. This spectrum with an average energy of 320 MeV was in good agreement with previous measurements obtained under similar operating conditions.

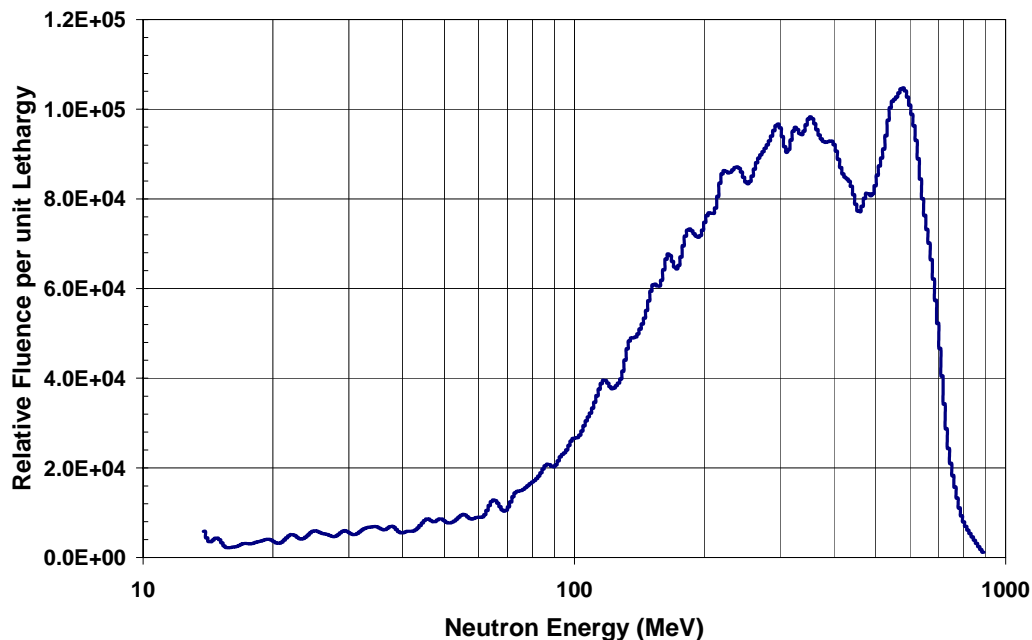


Figure 2. WNR neutron spectrum on 4FP15L

3 EXPERIMENTAL DETAILS

A detector probe consisting of a 1”x1” CsI(Tl) scintillator coupled to a Hamamatsu photomultiplier tube (R6094) was enclosed in a light tight aluminum housing. An external Ortec HV supply (model 566), typically set at 690v, was used to run the phototube. The anode signal from the PMT was passed through a current-to-voltage converter and sent via 50Ω co-axial cable to a Polaris™ digital spectrometer (X-ray Instrumentation Associates, Newark CA) running at a clock speed of 40MHz. The digitized data was relayed by USB cable to a laptop computer for display and storage. The laptop, through custom-written software, served to control the Polaris™ spectrometer. Spectrometer functions such as mode of operation, gain and threshold settings were accessed through this software.

The spectrometer was operated in either of two modes. The first was as a traditional multi-channel analyzer. Spectra were collected in this mode over 16K or 32K channels. Energy calibration was done using low energy gamma sources such as ²²Na and ⁶⁰Co. In the case of the UCL data, use was made of the fortuitous generation of 4.43 MeV gamma rays from the first excited state of ¹²C generated by the proton beam terminating in a carbon beam stop.

The second mode of operation, the so-called “List mode” involved the capture of individual waveforms that were stored on the laptop for later analysis. These digitized waveforms were analyzed off-line to generate plots of particle shape versus pulse energy.

Data was recorded at the UCL and WNR facilities but only the UCL data will be discussed, as the WNR data analysis is incomplete at this time.

4 MCNPX DETAILS

The MCNPX (version 2.5.e) [6] calculations were based on a bare 1”x1”CsI scintillator with a density of 4.51 g/cm³. A neutron beam at normal incidence and 1” in diameter was directed onto the front surface of the scintillator. The UCL (Figure 1) and WNR (Figure 2) spectra were randomly sampled in accordance with the relative fluence in each energy bin. Neutrons, photons, electrons, protons, deuterons, tritons, alphas and ³He particles were included on the mode card.

As charged particle and neutron cross section tables are not yet available for the target nuclei of interest (¹³³Cs and ¹²⁷I), models were used for particle generation and interaction. Version 2.5.e includes three high-energy physics models with which to simulate the interaction of neutrons with the CsI scintillator. The first two, Bertini [7] and ISABEL [8] are part of the LAHET Code System [9]. These intranuclear cascade (INC) models were used with their respective default settings. The standard multi-stage pre-equilibrium model was used to bridge the gap between the INC and evaporation regimes. In general, all three time/energy regimes can result in the emission of neutrons and charged particles. The models terminated by modeling the gamma de-excitation of the excited nucleus.

The third model used, CEM2k [10] is also based on the three-stage process *i.e.* INC, pre-equilibrium, and evaporation. By modifying the criteria used to control flow from one regime to the next, significant improvements relative to earlier versions of the code have been made. For our purposes, the most significant enhancement is the ability to extend the model to incident energies below 100MeV. Though it should be noted that the accuracy of any INC model is

limited below about 50MeV, since one of the underlying assumptions is that the projectile energy is many times the nucleon binding energy.

Each of the three models was applied to calculate two quantities of interest; charged particle yield and pulse height spectra that could be directly compared to experimental results. The yield data is important from the point-of-view of detector efficiency as the scintillator must be large enough to give adequate sensitivity and stopping power but, on the other hand, this concern must be balanced with the desire to make the instrument package as lightweight as possible.

Pulse height spectra were generated using the PHL option on the FT card associated with F8 (pulse height) tallies. By specifying the tally cell (*i.e.* CsI scintillator volume) and the particle(s) of interest on the PHL card, a pulse height spectrum for one or more particle types could be generated. Along each incremental track length, the energy deposited in the tally cell (F6-type tally) was folded with differential light curve data (dL/dE) stored in a particle-specific DE/DF data array. At the end of the history, the total light output was calculated by summing the track-by-track contributions.

Light curves (dL/dE) were calculated for each particle of interest using Birk's formula [11] as shown in Equation 1, where S is

$$dL/dE = S / (1 + kB \cdot dE/dX) \quad (1)$$

the scintillation efficiency, kB the quenching parameter and dE/dX the specific energy loss. The value of S becomes unity by definition when the scintillator is calibrated in terms of electron equivalent energy (MeVee) using gamma sources. The value of kB can be determined empirically from the pulse height defect observed with charged particle spectra when the particle energy is either known or can be accurately calculated.

5 RESULTS

5.1 Experimental Data

5.1.1 UCL results

Figure 3 shows the pulse shape discrimination versus light output plot obtained for the quasi-monoenergetic 33MeV neutron beam. A pulse identification index (PID) was calculated by dividing the signal integrated over the initial 1 μ s of the pulse by the total light output. There is a clear separation of particle types and the quadrant defined by $PID > 0.52$ and pulse height > 6 MeVee uniquely designates charged particle events. Protons, deuterons and alphas dominate this charged particle region but the majority of the 76K events comprising this plot are low energy gamma rays.

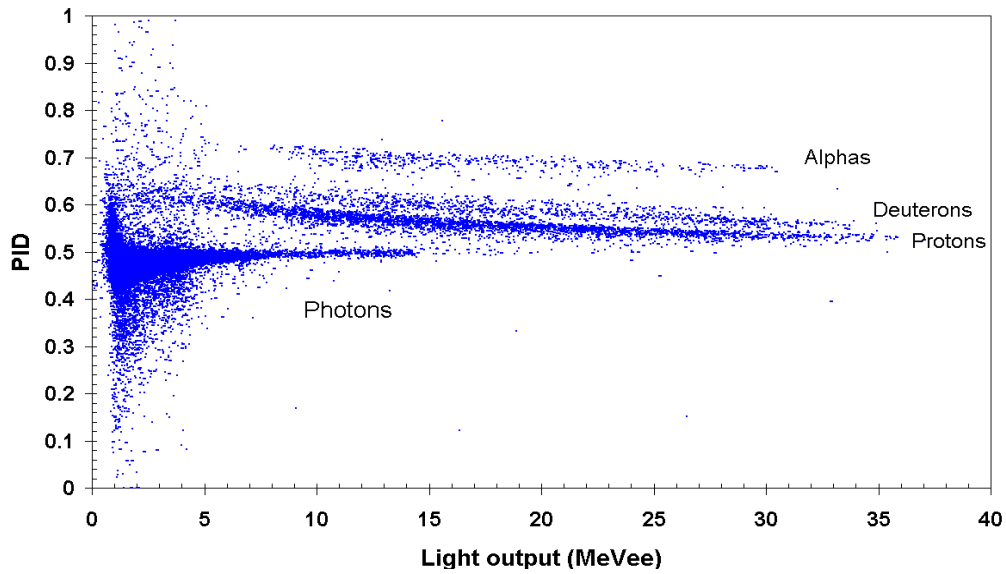


Figure 3. Pulse identification index as function of pulse height for 33MeV UCL beam

The PID plot obtained for the 60MeV beam is shown in Figure 4 where a high degree of particle discrimination was again observed.

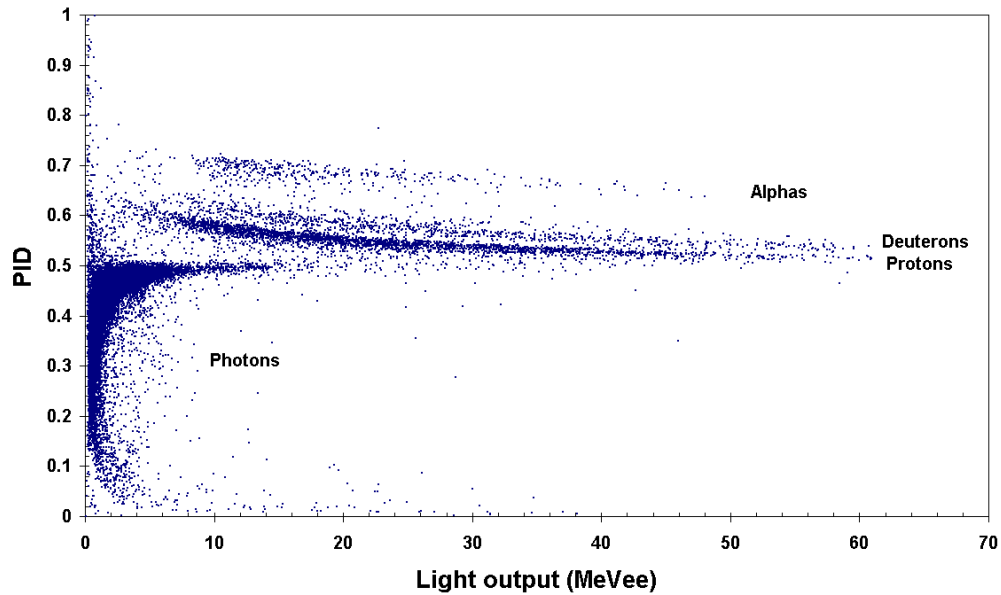


Figure 4. Pulse identification index as function of pulse height for 60MeV UCL beam

By summing the events associated with each particle type and dividing by the total delivered fluence, absolute yields for protons, deuterons and alphas were calculated. This fluence was dead time corrected and, in addition, a $1/r^2$ correction was applied to account for the difference between the measurement location and the position used by the metrology instrumentation. The yield results for 33 and 60MeV beams are shown in Table 1 where a lower threshold of 6MeVee was applied in summing the charged particle yields. The 33MeV yields were better determined as the uncertainty associated with the dead time correction was higher for the 60MeV data. The column marked “others” represents those events not clearly associated with any of the three main charged particle streams identified in Figures 3 and 4.

Table 1. Absolute number of charged particle events above 6MeVee per unit fluence for a 1"x1" CsI(Tl) scintillator

Energy (MeV)	Protons	Deuterons	Alphas	Others	Total
33	$1.84(7) 10^{-2}$	$5.71(23) 10^{-3}$	$2.76(11) 10^{-3}$	$3.83(15) 10^{-3}$	$3.07(12) 10^{-2}$
60	$5.0(3) 10^{-2}$	$1.6(1) 10^{-2}$	$7.9(5) 10^{-3}$	$3.4(2) 10^{-3}$	$7.7(3) 10^{-2}$

The number in parenthesis represents the statistical uncertainty (1σ) in the last digit(s)

5.2 MCNPX Particle Yields

5.2.1 Monoenergetic neutron beams

MCNPX was used initially used to calculate particle yields for a broad parallel beam of monoenergetic neutrons normally incident on the front face of bare CsI scintillators. Simulations were run using each of the high-energy physics models for right circular cylindrical-shaped scintillators 1"x1", 1.5"x1.5" and 2"x2" in dimension.

Figure 5 plots the neutron and proton yields per source neutron as a function of incident neutron energy for a 1"x1" CsI crystal. The runs at each neutron energy were long enough to ensure that the statistical uncertainty (1σ) in yield was no more than 2%. None of the models predicted charged particle production below a threshold of 20MeV.

It can be seen in Figure 5 that the most prevalent particle emitted from the nucleus (excluding photons) are neutrons for which all the models give comparable estimates of yield. The proton yields are in reasonable agreement, with the ISABEL-based prediction agreeing with the Bertini model at low energy and converging with the CEM2k result at 800MeV.

The corresponding plot for deuterons and alpha particles is shown in Figure 6. The alpha production yields are in fair agreement but the CEM2k model predicts a significantly higher deuteron yield than the other models at all energies.

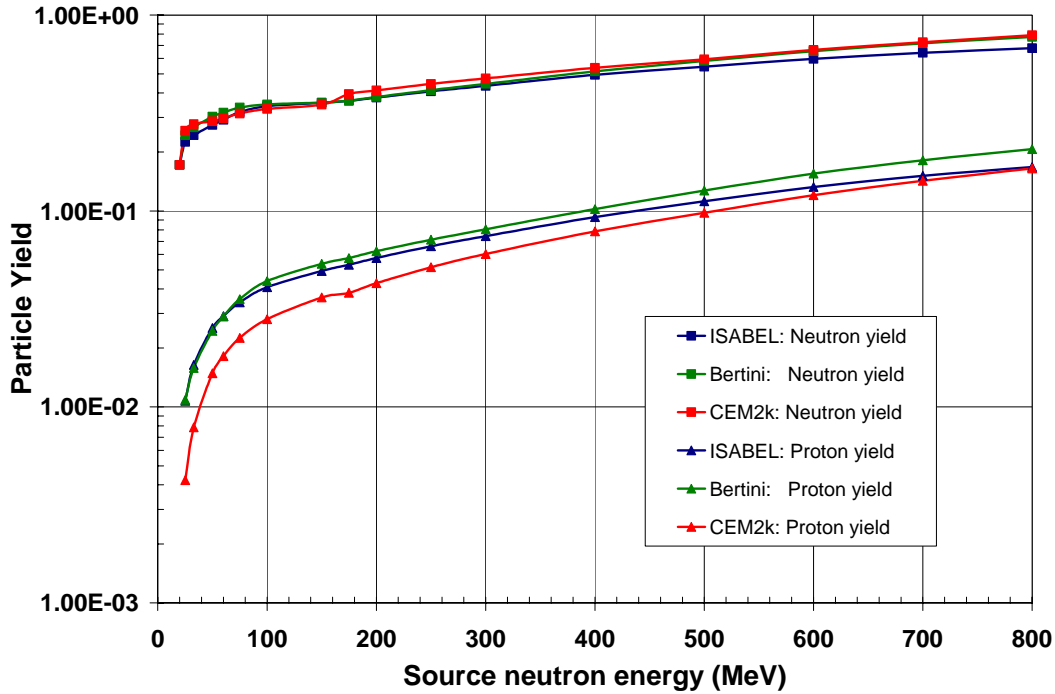


Figure 5. MCNPX calculation of neutron and proton yields for a 1''x1'' CsI scintillator per source neutron

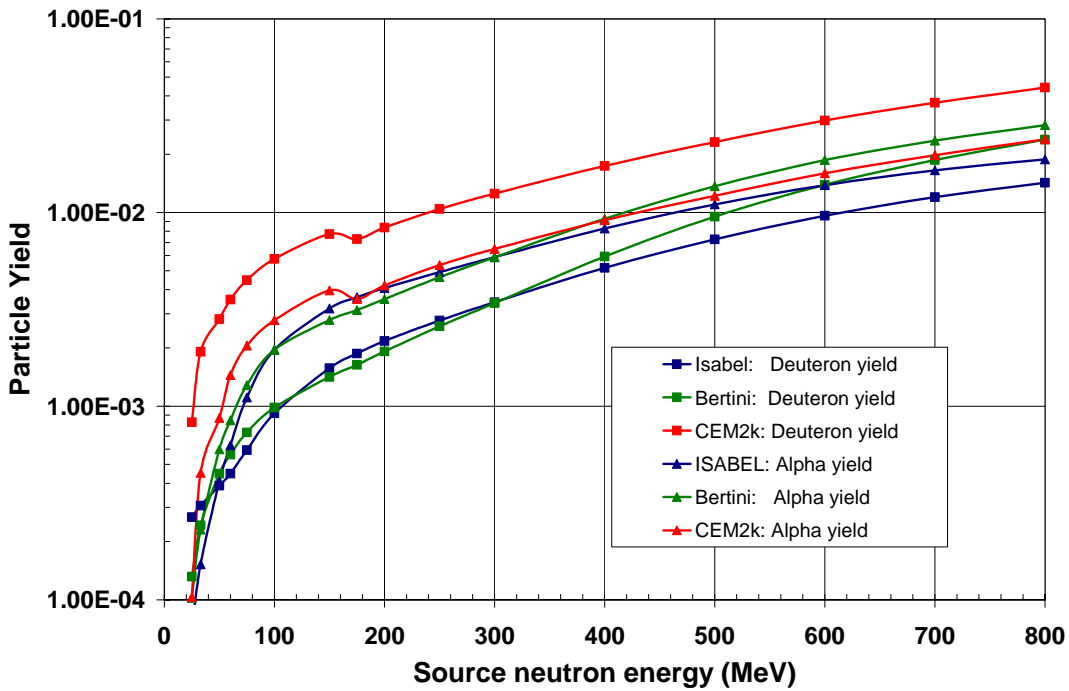


Figure 6. MCNPX calculation of deuteron and alpha yields for a 1''x1'' CsI scintillator per source neutron

It is also interesting to note that the CEM2k model predicts deuteron production is always favoured over alpha production while the reverse is true for the ISABEL and Bertini (for $E_n < 600\text{MeV}$) models at incident energies above about 60MeV. The CEM2k-predicted yields show an abrupt change between 150 and 175MeV for both particle types. This anomalous feature is also present, though to a much smaller extent, in the neutron and proton production data displayed in Figure 5.

5.3 MCNPX calculation of particle yields at neutron facilities

5.3.1 UCL beams

MCNPX-generated pulse height spectra in a 1"x1" CsI crystal using the 33 and 60MeV UCL spectra were done using each of the three models as will be discussed in section 5.4. From these spectra, charged particle yields were calculated. To facilitate comparison with experimental data, only particles generating pulse heights greater than 6MeVee were included in the yield determination as summarized in Table 2.

Table 2. Model predictions of particles per unit fluence generating pulse heights above 6MeVee

	$E_n=33\text{MeV}$			$E_n=60\text{MeV}$		
Model	Protons	Deuterons	Alphas	Protons	Deuterons	Alphas
CEM2k	$1.91(4) \cdot 10^{-2}$	$4.5(2) \cdot 10^{-3}$	$7.6(6) \cdot 10^{-4}$	$5.22(9) \cdot 10^{-2}$	$1.12(4) \cdot 10^{-2}$	$3.8(2) \cdot 10^{-3}$
ISABEL	$4.06(9) \cdot 10^{-2}$	$8(1) \cdot 10^{-4}$	$3.2(4) \cdot 10^{-4}$	$8.6(2) \cdot 10^{-2}$	$1.4(2) \cdot 10^{-3}$	$1.6(1) \cdot 10^{-3}$
Bertini	$3.90(6) \cdot 10^{-2}$	$5.5(6) \cdot 10^{-4}$	$4.6(4) \cdot 10^{-4}$	$8.4(2) \cdot 10^{-2}$	$1.5(3) \cdot 10^{-3}$	$2.2(2) \cdot 10^{-3}$

Number in parenthesis is the statistical uncertainty corresponding to 1σ in the last quoted digit

The results shown in Table 2 can be compared with the experimental data shown in Table 1. The CEM2k model gives the best agreement for all particle types at both energies with the proton yield being in particularly good agreement. All the models under predict the production of deuterons and alphas, which is partially due to the 20MeV production threshold used in the models. However, the experimental data does lend support to the relatively high deuteron yield predicted by the CEM2k model as shown in Figure 6.

5.3.2 WNR beam

Table 3 presents particle yields per source neutron, using the spectrum shown in Figure 2, for a broad parallel beam incident on the entrance face of a 1"x1" CsI scintillator. Except for deuteron yields, the models are in good agreement. The statistically uncertainty in the yields is no more than 0.5%.

Table 3. MCNPX predictions of particle yields per unit fluence for a 1"x1" CsI scintillator in WNR beam

Model	Neutrons	Photons	Protons	Deuterons	Alphas
CEM2k	7.519	2.297	$3.31 \cdot 10^{-1}$	$7.50 \cdot 10^{-2}$	$3.90 \cdot 10^{-2}$
ISABEL	7.326	2.190	$3.99 \cdot 10^{-1}$	$2.19 \cdot 10^{-2}$	$3.43 \cdot 10^{-2}$
Bertini	7.448	2.236	$4.46 \cdot 10^{-1}$	$2.74 \cdot 10^{-2}$	$4.05 \cdot 10^{-2}$

5.4 MCNPX-Calculation of Pulse Height Spectra and Comparison with Experiment

Figure 7 displays the spectrum of proton, deuteron and alpha particle energies predicted by the CEM2k code for the 60MeV UCL beam. This spectrum was generated by starting source neutrons at the center of a 10cm sphere of CsI to ensure total energy absorption of the spallation products emitted and, simultaneously, setting all dL/dE values to unity. The spectra shown in

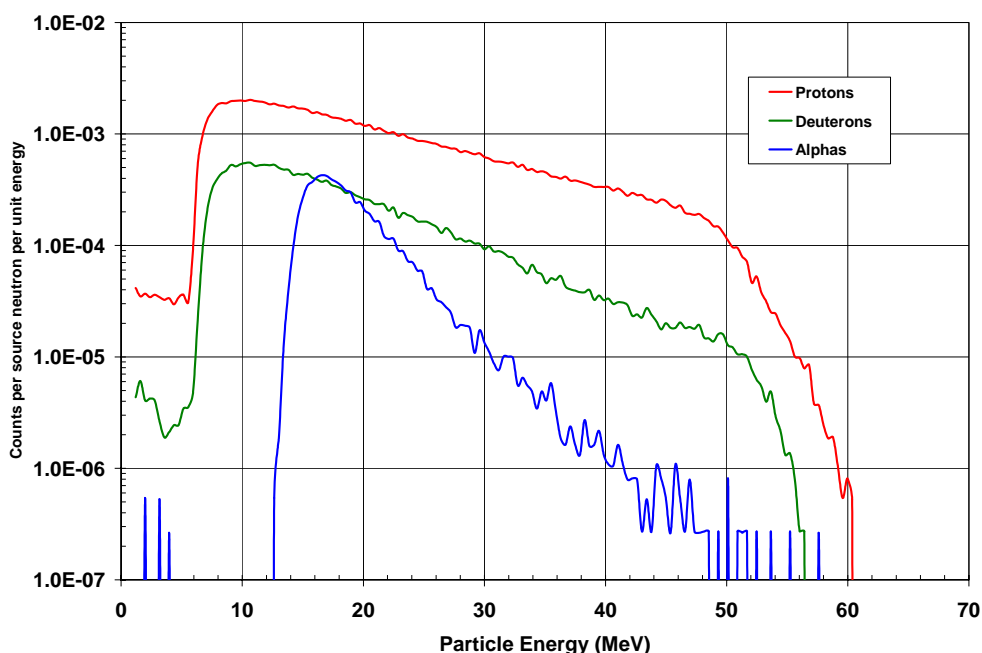


Figure 7. Spectrum of particle energies predicted using the CEM2k model using the 60MeV UCL beam as the source term

Figure 7 are similar in appearance to spectra calculated for neutrons on ^{133}Cs as given in reference 12. Based on the data displayed in Figure 7, average particle energies of 20.3MeV, 17.9MeV and 20.4MeV were calculated for protons, deuterons and alphas respectively.

The individual spectra shown in Figure 7 can be compared to the data shown in Figure 4; the end point energies shown in Figure 7 for each particle stream are in good agreement with the

corresponding values shown in Figure 4. This good correlation between particle energy and light output is a manifestation of the relatively low specific energy loss for these high-energy particles. Though not shown in Figure 7, the ISABEL and Bertini models predicted very similar energy distributions that differed significantly from the CEM2k-based prediction. The ISABEL and Bertini models gave proton spectra that extended to higher energy, approaching the maximum neutron energy. However, both these models predicted a relatively soft alpha spectrum that extended to only 25 MeV, in stark contrast to the measured pulse height spectrum that continues to about 50 MeVee (Figure 4). Here, the CEM2k model result, as shown in Figure 7, shows more consistency with the experimental alpha spectrum.

Based on a re-analysis of low energy alpha pulse height data recorded using CsI(Tl) [13], a value of $7 \times 10^{-4} \text{ g MeV}^{-1} \text{ cm}^{-2}$ for the quenching parameter defined in Equation 1 was calculated. Equation 1 was then applied to generate differential light curves for all the particles on the mode card. Based on these curves, pulse height data were calculated assuming a broad parallel beam incident on 1"x1" CsI scintillator with the 33MeV and 60MeV UCL spectra as source terms. The data shown in Table 2 was derived from these spectra.

Figure 8 shows an absolute comparison between the measured UCL spectrum at 60MeV and the MCNPX-generated spectra from each of the physics models.

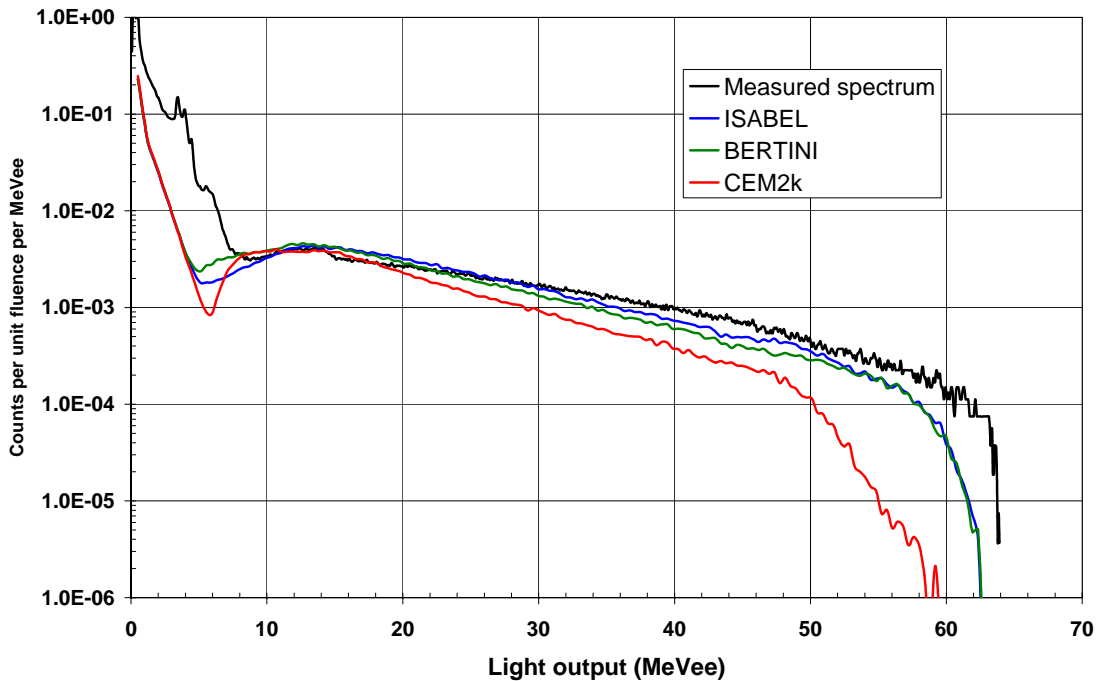


Figure 8. Comparison of measured and model predictions of 1''x1'' CsI scintillator pulse height spectrum in 60MeV UCL beam

Figures 9-11 show a detailed comparison of the measured and CEM2k-predicted pulse height spectra for protons, deuterons and alphas respectively for the 60MeV UCL beam. The measurement data was extracted from the spectral data displayed in Figure 4. The calculated

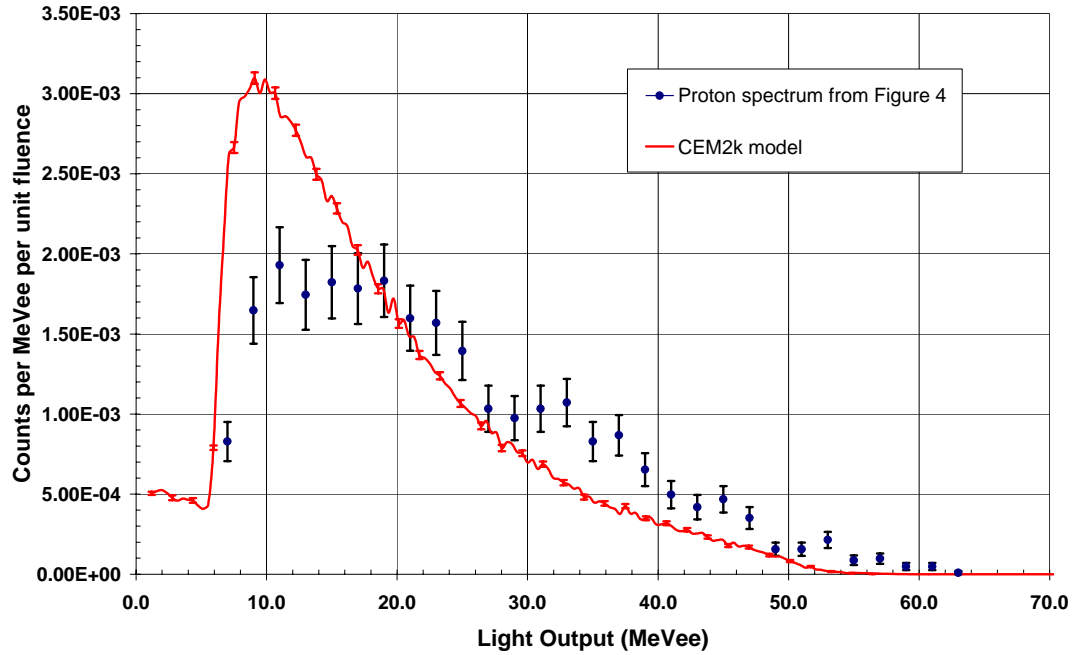


Figure 9. Absolute comparison of measured and CEM2k model calculation of proton pulse height spectrum for 1x1 CsI scintillator in 60MeV UCL beam

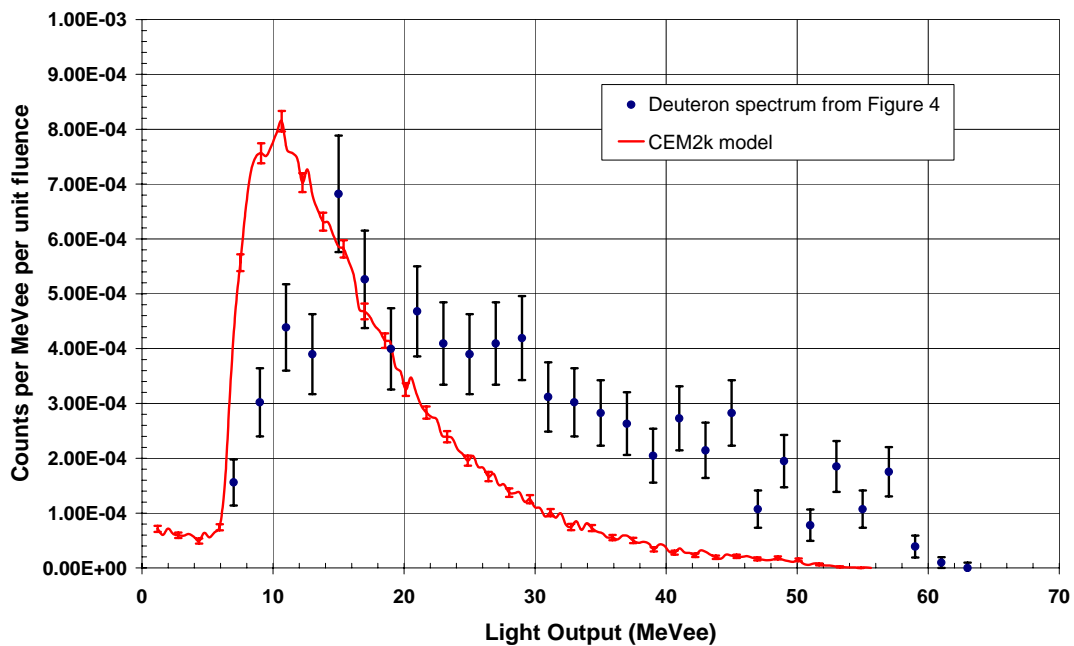


Figure 10. Absolute comparison of measured and CEM2k model calculation of deuteron pulse height spectrum for 1x1 CsI scintillator in 60MeV UCL beam

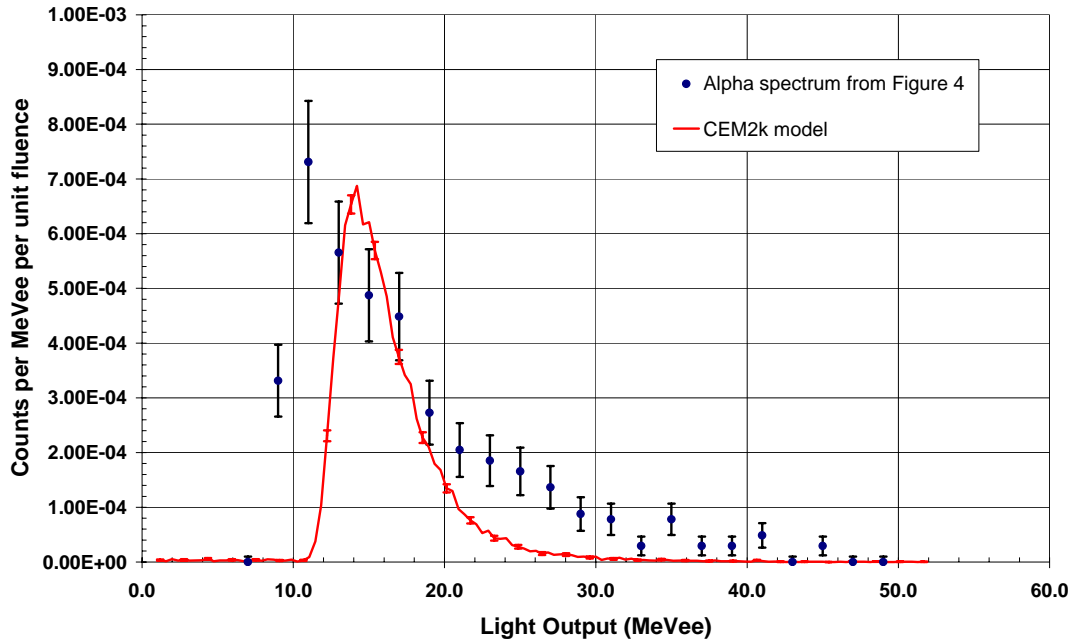


Figure 11. Absolute comparison of measured and CEM2k model calculation of alpha pulse height spectrum for 1x1 CsI scintillator in 60MeV UCL beam

proton and deuteron spectra are skewed towards lower energy relative to the measured spectrum. However, the integrated particle yields, particularly for protons, are in good agreement as indicated by the data in Tables 1 and 2. The error bars shown in Figures 9-11 correspond to $\pm 1\sigma$ based on the respective statistical uncertainties in the measured and calculated spectra.

6 CONCLUSIONS

The high energy physics models bundled with MCNPX have been used to model the interaction of high-energy neutrons in a CsI scintillator with the eventual aim of generating a reliable set of response functions. It is vital that these theoretical calculations be validated using empirical data. Comparison with measurements obtained using quasi-monoenergetic neutrons at nominal beam energies of 33 and 60MeV suggest that the CEM2k model performs better at these relatively low energies than the LAHET-based models in terms of predicting particle yields. However, the spectral shape of the theoretical pulse height data show pronounced differences with the measured spectra.

7 ACKNOWLEDGMENTS

We would like to thank Peter Grudberg and Anthony Fallu-Labruyere of X-ray Instrumentation Associates for their help in obtaining the experimental data. Thanks are also due to Ralf Nolte and J.P. Meulders for their help at UCL. We acknowledge the assistance of Bob Haight, Matt Devlin, John O'Donnell, Nick Fotiadis and Leonard Romero in the WNR

experiments. Discussions with Greg McKinney and Stephan Mashnik have been beneficial. We are also grateful for financial support from the Technical Development, Evaluation and Application program administered by the HSR division at LANL.

8 REFERENCES

1. T.D. McLean, R.H. Olsher and R.T. Devine, “Development of a portable high-energy neutron spectrometer”, *Radiation Protection Dosimetry*, **110**, pp.219-222 (2004)
2. C.M. Bartle and R.C. Haight, “Small inorganic scintillators as neutron detectors”, *Nucl. Instrum. Meth.*, **A422**, pp.54-58 (1999)
3. A.S. Formichev and 14 others, “The response of a large CsI(Tl) detector to light particles and heavy ions in the intermediate energy region”, *Nucl. Instrum. Meth.*, **A344**, pp.378-383 (1994)
4. W. Skulski and M. Momayezi, “Particle identification in CsI(Tl) using digital pulse shape analysis”, *Nucl. Instrum. Meth.*, **A458**, pp.759-771 (2001)
5. R. Nolte and 9 others, “High-energy neutron reference fields for the calibration of detectors used in neutron spectrometry”, **A476**, pp.369-373 (2002)
6. L.S. Waters, Ed., “MCNPX – a general code for radiation transport”, Version 2.5e, Los Alamos National Laboratory, Los Alamos, USA. February 2004
7. H.W. Bertini, “Intra-nuclear cascade calculation of the secondary nucleon spectra from nucleon-nucleus interactions in the energy range 340 to 2900 MeV and comparison with experiment”, *Phys. Rev.*, **188**, pp.1711-1730 (1969)
8. Y. Yariv and Z. Fraenkel, “Intranuclear cascade calculation of high-energy heavy-ion interactions”, *Phys. Rev. C*, **20** pp.2227-2243 (1979)
9. R.E. Prael and H. Lichtenstein, “User guide to LCS: The LAHET code system”, LA-UR-89-3014, Los Alamos National Laboratory, Los Alamos (1989)
10. S.G. Mashnik and A.J. Sierk, “Recent developments of the cascade-exciton model of nuclear reactions”, LA-UR-01-5390, Los Alamos National Laboratory, Los Alamos (2001)
11. J.B. Birks, *The theory and practice of scintillation counting*, Pergamon Press, Oxford UK (1964)
12. Y.L. Parenova and O.V. Fotina, “Spectra of light particles and gamma rays in neutron-induced reactions in the energy range from 6 to 100MeV”, *Phys. At. Nucl.*, **56**, pp1002-1008 (1993)
13. M.L. Halbert, “Fluorescent response of CsI(Tl) to energetic nitrogen ions”, *Phys. Rev.*, **107**, pp647-649, (1957)